



Spreading Factor Allocation in LoRaWAN for Reliability and Delay-Constrained Smart Metering Applications

Thiago Allisson Ribeiro da Silva   [Universidade Federal do Piauí, Instituto Federal do Maranhão | thiago.allisson@ufpi.edu.br]

Geraldo A. Sarmento Neto  [Universidade Federal do Piauí | geraldosarmento@ufpi.edu.br]

Luís H. Oliveira Mendes  [Universidade Federal do Piauí | luishenriqueom@ufpi.edu.br]

Pedro F. Ferreira Abreu  [Universidade Federal do Piauí | pedroffda@ufpi.edu.br]

Fernando J. Vieira Santos  [Universidade Federal do Piauí | fernando.vieira@ufpi.edu.br]

José Valdemir dos Reis Jr  [Universidade Federal do Piauí | valdemirreis@ufpi.edu.br]

 Universidade Federal do Piauí, Campus Universitário Ministro Petrônio Portella - Ininga, Teresina - PI, 64049-550.

Received: 15 April 2025 • **Accepted:** 26 August 2025 • **Published:** 14 October 2025

Abstract Long Range Wide-Area Network (LoRaWAN) is a prominent IoT technology, and one of its operational parameters that significantly influences reliable transmission and packet delivery delay is Spreading Factor (SF). In this context, this paper develops a Spreading Factor Allocation scheme, named Delay and Reliability-aware Spreading Factor Allocation (DR-SFA), and evaluates it through simulations in comparison with four related solutions: Initial - Spreading Factor Allocation (I-SFA), Adaptive Data Rate (ADR), I-SFA+ADR, and Collision-Aware Adaptive Data Rate (CA-ADR). The simulated scenarios model an Advanced Metering Infrastructure (AMI) executing Interval Meter Reading (IMR) and Power-Control Command (PCC) applications, with 200 to 1000 Smart Meters (SMs) distributed across an area of 56.25 km². The results demonstrate that DR-SFA outperforms the alternative solutions by reducing the number of required Data Aggregation Points (DAPs) by up to 92.86%, while meeting the reliability and maximum delay requirements of the tested applications. Furthermore, DR-SFA successfully receives packets from meters located up to 2197.56 meters away in the scenario with 200 SMs, and achieves a Packet Delivery Ratio (PDR) of 99.49%, while also decreasing packet loss due to interference by 83.84% compared to ADR, and packet loss due to under sensitivity by 53.96% compared to I-SFA+ADR, in the scenario with 1000 SMs.

Keywords: Delay, LoRaWAN, Reliability, Smart Metering, Spreading Factor Allocation.

1 Introduction

The traditional Electric Power System (EPS) is being transformed into a Smart Grid (SG), and one of the essential steps in this process is the deployment of the AMI system in the power grid [Marques *et al.*, 2023]. For this purpose, SMs must be installed on the consumer side to sense variables related to electricity consumption, such as active power and current values [Veloso *et al.*, 2021]. Furthermore, SMs must be equipped with communication interfaces that enable the transmission of the sensed data to DAPs, which act as base stations responsible for receiving packets from various SMs and forwarding them to control centers managed by the electric utility company [Khan *et al.*, 2021].

The AMI system requires that the communication technology employed be capable of fulfilling the Quality of Service (QoS) requirements of the applications being executed, particularly with respect to packet delivery reliability rate and maximum communication delay [Khan *et al.*, 2022]. In line with these requirements, the evolution of the IoT paradigm has driven the development of wireless technologies such as LoRaWAN, which enables long-range signal transmission with high robustness while maintaining low deployment and maintenance costs [Júnior *et al.*, 2023]. Consequently, it has been widely adopted in scenarios such as precision agriculture [Alumfareh *et al.*, 2024] and industrial automa-

tion [Kumar *et al.*, 2023].

In this way, the power sector can benefit from the LoRaWAN standard, as this technology enables the construction of a communication infrastructure with low investment and is also capable of transmitting the data sensed by the SMs to DAPs located several kilometers away [Zain *et al.*, 2022]. Furthermore, energy distributors can use the collected data, for example, to provide a continuous supply of high-quality electricity and to manage power system assets more efficiently. However, an infrastructure based on LoRaWAN requires proper planning to ensure that the QoS requirements of the applications to be executed are met [Da Silva *et al.*, 2024].

The LoRaWAN technology has several operational parameters, and one of the most critical is SF. For this reason, various Spreading Factor Allocation (SFA) schemes have been proposed [Abd Elkarim *et al.*, 2022]. However, there is still a lack of a solution capable of balancing the network traffic load among the different SFs, while assigning the appropriate SFs to devices according to the delay and transmission success rate requirements of the applications in operation. In this context, this paper proposes an SFA scheme, named DR-SFA, aimed at ensuring that the requirements of AMI applications, such as IMR and PCC, are met. These applications transmit energy consumption data and load control signals, respectively, and require high reliability and low delay [Khan *et al.*,

2023].

The scheme proposed in this paper is compared through simulations with four alternative solutions presented in the literature: I-SFA [Farhad *et al.*, 2020b], ADR [Farhad *et al.*, 2020b], I-SFA+ADR [Soto-Vergel *et al.*, 2023], and CA-ADR [Marini *et al.*, 2020]. The simulated scenarios consist of an urban environment of 56.25 km² [Farhad *et al.*, 2020c], with 200 to 1000 SMs [Neto *et al.*, 2024] implemented as LoRaWAN End Devices (EDs), as described in [Enriko *et al.*, 2021] and randomly distributed throughout the network [Magrin *et al.*, 2020], while DAPs are configured as LoRaWAN Gateways (GWs), following the modeling also established in [Enriko *et al.*, 2021], and the positions of the DAPs are defined using the K-Means algorithm, in an approach similar to that described in [Loh *et al.*, 2023].

The main contributions of the proposed scheme can be summarized as follows:

- Reduction in the number of DAPs, minimizing the deployment and maintenance costs of the communication infrastructure;
- Appropriate distribution of SFs, ensuring that the QoS requirements of the applications are met and that the Time on Air (ToA) of packets complies with their respective delay constraints;
- SFA strategy tailored for AMI applications with heterogeneous QoS requirements, adjusting the SF assigned to each SM according to the specific characteristics of the applications;
- More efficient communication, improving the PDR as well as the delivered signal quality, and ensuring successful packet reception from SMs located farther from the DAPs when compared to state-of-the-art solutions.

The remainder of this work is structured as follows. Section 2 presents the theoretical foundation: it describes LoRaWAN technology and the importance of SF, discusses SFA schemes and the ADR standard, explains the transmission success probability in LoRaWAN, describes the characteristics of AMI, and introduces the K-Means algorithm. Section 3 compares related work with the solution proposed in this paper. Section 4 provides a detailed description of the proposed scheme. Section 5 outlines the applied methodology. Section 6 presents and discusses the results. Finally, Section 7 concludes the work and outlines future research directions.

2 Background

This section initially presents the LoRaWAN technology, describing its operation, operational parameters, and architecture. It also discusses the influence of the SF parameter on network performance, introduces the I-SFA allocation scheme – one of the components of the proposed DR-SFA scheme –, details the transmission success probability formulation used to support SF allocation, and explains the ADR standard. Subsequently, the AMI system and its applications are described. Finally, the K-Means clustering algorithm applied to determine the placement of DAPs is presented.

2.1 LoRaWAN

LoRaWAN is a wireless IoT technology that belongs to the Low-Power Wide-area Network (LPWAN) class, characterized by low deployment cost, long communication range, and low power consumption [Magrin *et al.*, 2020]. This technology has been applied in various scenarios, such as precision agriculture [Alumfareh *et al.*, 2024], smart homes [Abd Elkarim *et al.*, 2022], smart cities [Zain *et al.*, 2022], industrial automation [Kumar *et al.*, 2023], and smart metering [Da Silva *et al.*, 2024]. Its architecture is described in the specification presented in [LoRa Alliance, 2017] and illustrated in Figure 1, operating under a star-of-stars topology [Jouhari *et al.*, 2023], and is composed of the following components:

- EDs: devices that run sensing applications and transmit their data through the LoRaWAN channel;
- GWs: devices that act as base stations, receiving data sent by the EDs over the LoRaWAN channel and forwarding it to external networks;
- Network Server (NS): component that receives the data forwarded by the GWs in a network external to the LoRaWAN standard;
- Application Server (AS): component that receives data from the NS, stores it in databases, and provides the data to applications, which in turn deliver services to end users.

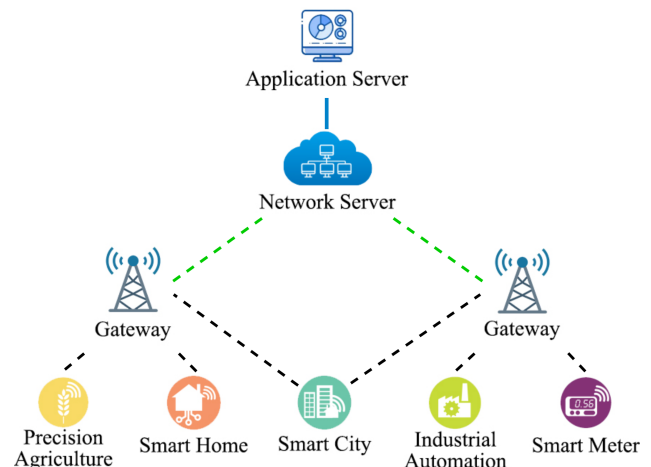


Figure 1. LoRaWAN Network Architecture.

According to the description presented in [Al-Sammak *et al.*, 2024], LoRaWAN devices apply several communication parameters, among which the main ones are:

- SF: ranges from 7 to 12, where higher values allow the signal to reach longer distances, reduce the minimum sensitivity (in dBm) required for data reception by GWs, and consequently enable the demodulation of packets with lower received power. However, higher SFs also consume more energy than lower ones and reduce the size of packets that can be transmitted;
- Transmission Power (TP): transmission power levels, typically ranging from 2 to 14 dBm for EDs in the European frequency band, which is the configuration adopted in this paper. In contrast, the maximum TP can reach up

to 16 dBm in some Asian regions and up to 30 dBm in the United States;

- Bandwidth: the amount of spectrum allocated for channel transmission, which can be configured to 125, 250, or 500 kHz, with 125 kHz being the most commonly used setting;
- Coding Rate (CR): the number of control bits used for error correction, represented as a fraction and ranging from $\frac{4}{5}$ to $\frac{4}{8}$, where $\frac{4}{5}$ corresponds to 1 control bit for every 4 data bits, and $\frac{4}{8}$ to 4 control bits for every 4 data bits.

The SF parameter is one of the most critical in LoRaWAN networks, as it influences the transmission range, the ability to correctly demodulate packets, and the number of bits that can be transmitted by the EDs [Abd Elkarim *et al.*, 2022]. An ED operating with SF7 has a reduced signal transmission range and can transmit packets with a payload of up to 222 B. In addition, GWs can successfully receive packets transmitted with this SF at a received signal strength of up to -130.0 dBm and a minimum Signal-to-Noise Ratio (SNR) of -7.5 dB, as established in the technical specification of the LoRaWAN technology presented in the SX1301 datasheet [Semtech, 2017] and shown in Table 1. In contrast, an ED configured with SF12 can transmit payloads of up to 51 B and benefits from an extended transmission range, with GWs able to correctly demodulate packets at sensitivity levels as low as -142.5 dBm and an SNR threshold of -20.0 dB [Semtech, 2017], also presented in Table 1.

Table 1. Sensitivity, SNR Threshold, and Data Payload per SF.

SF	Sensitivity (dBm)	SNR Threshold (dB)	Data (B)
SF7	-130.0	-7.5	222
SF8	-132.5	-10.0	222
SF9	-135.0	-12.5	115
SF10	-137.5	-15.0	51
SF11	-140.0	-17.5	51
SF12	-142.5	-20.0	51

Another important characteristic of the LoRaWAN network is the ToA, which refers to the total duration of the LoRaWAN frame transmission over the channel [LoRa Alliance, 2017], and is calculated using Equation 1:

$$ToA = T_{preamble} + T_{payload} \quad (1)$$

where $T_{preamble}$ is the duration of the preamble symbol and $T_{payload}$ is the duration of the payload of the frame.

ToA of the preamble depends on the number of symbols in the preamble, $n_{preamble}$, and is obtained using Equation 2. For the EU-868 region, which includes Europe, $n_{preamble} = 8$ [Marini *et al.*, 2022].

$$T_{preamble} = (n_{preamble} + 4.25) \cdot T_{symbol} \quad (2)$$

In turn, the duration of the payload [LoRa Alliance, 2017], $T_{payload}$, is calculated using Equation 3:

$$T_{payload} = n_{payload} \cdot T_{symbol} \quad (3)$$

where $n_{payload}$ is the number of symbols in the payload of the link layer data unit, calculated using Equation 4:

$$n_{payload} = \max \left(\left\lceil \frac{8 \cdot PS - 4 \cdot SF + 28 + 16 \cdot CRC - 20 \cdot H}{4 \cdot (SF - 2 \cdot LDRO)} \right\rceil \cdot (CR + 4), 0 \right) \quad (4)$$

where the first parameter is Packet Size (PS); Cyclic Redundancy Check (CRC) is the packet integrity verification mechanism, enabled when $CRC = 1$ and disabled when $CRC = 0$; $H = 1$ when the header is enabled, and $H = 0$ when no header is present; $LDRO = 1$ when Low Data Rate Optimization (LDRO) is enabled, and $LDRO = 0$ when it is disabled.

2.1.1 Spreading Factor Allocation

SF plays a fundamental role in LoRaWAN networks, and an appropriate allocation scheme is essential for network performance. EDs running applications with stricter delay requirements or operating in real time should use lower SFs, with a ToA that allows for acceptable communication latency [Wei *et al.*, 2023]. Various strategies for SFA exist, ranging from simple approaches that assign SFs to 7 or 12, to more sophisticated schemes that consider minimum reception sensitivity or maximum transmission range [Farhad *et al.*, 2020b].

Sensitivity-based allocation schemes are simple and have the advantage of verifying whether the received power at the GWs is within the reception sensitivity threshold of a given SF, thus reducing packet loss due to under sensitivity [Farhad *et al.*, 2020c]. Meanwhile, allocating only SF7 results in lower transmission delay, improved energy efficiency, and reduced coverage. On the other hand, the exclusive use of SF12 extends coverage, increases signal robustness, and leads to higher energy demand. Lastly, range-based schemes determine the maximum distance at which a given SF can be used based on channel conditions and are less straightforward to implement [Loh *et al.*, 2023].

An example of a sensitivity-based scheme that serves as the foundation for the development of the scheme proposed in this paper is I-SFA. This scheme is presented in Algorithm 1 and determines, through the *MaxPrAndBestGw* function, the maximum received power, P_r^{max} , and the Gateway GW_i that receives the signal with the highest power – the best GW – for a packet transmitted by ED_j , as shown in the first line of the algorithm. The power received by GWs is calculated using Equation 5:

$$P_r = P_t - P_l \quad (5)$$

where P_r is the received power, P_t is the transmission power of the packet, set to 14 dBm, and P_l correspond to the propagation and shadowing losses experienced by the packet until it reaches the GW.

Next, the scheme checks, in lines 2 to 6, the sensitivity thresholds, denoted as $S_{Rx}[k]$, to determine the range in which P_r^{max} lies, ensuring that $P_r^{max} > S_{Rx}[k]$, and assigns the corresponding SF, SF_k , to ED_j . If none of the conditions are satisfied, SF12 is assigned. Thus, for example, if $P_r^{max} > -130$ dBm, SF7 is selected, as established in the SX1301 datasheet [Semtech, 2017] and presented in Table 1.

Algorithm 1: I-SFA Algorithm.

Input: ED to configure SF: ED_j , set of GWs: G , SF sensitivities in dBm: S_{Rx}

```

1  $P_r^{max}, GW_i \leftarrow \text{MaxPrAndBestGw}(ED_j, G)$ 
2  $SF_k \leftarrow 12$ 
3 for  $k \leftarrow 0$  to 5 do
4   if  $P_r^{max} > S_{Rx}[k]$  then
5      $SF_k \leftarrow k + 7$ 
6   break
7 return  $ED_j, P_r^{max}, SF_k, GW_i$ 
```

2.1.2 Adaptive Data Rate

The ADR standard performs dynamic adjustments to the SF and TP of the EDs based on link conditions, eliminating the need for manual configuration. Under poor signal conditions, ADR can increase the SF and TP, ensuring that communication remains functional. Thus, the use of ADR can enhance signal range and reliability. However, its operation relies on several previous transmissions to determine the necessary adjustments and sends downlink messages to the EDs to modify their configurations, which increases the network traffic load [Farhad et al., 2020b].

Algorithm 2 describes the operation of the ADR standard. It assumes that the initial SF, SF_k , is 12, and the initial TP, TP_k , is 14 dBm. In the first step, the maximum SNR value, SNR_{max} , is computed using the function GetMaxSnr , which takes as input the ED to be configured, ED_j ; the history of stored SNR values, S ; and N , the number of most recent values to be considered when calculating SNR_{max} , typically set to 20 [Soto-Vergel et al., 2023]. Then, in line 2, the minimum SNR, SNR_{min} , for SF_k is identified from Γ , which stores the sensitivity thresholds for the SFs in dB [Farhad et al., 2020c].

Since SF_k is initially 12, the value of -20.0 dB is assigned to SNR_{min} . Afterward, SNR_{margin} and the number of adjustment steps, N_{step} , are calculated, with N_{step} corresponding to the average between SNR_{max} , SNR_{min} , and 10, thus resulting in $N_{step} = \frac{SNR_{margin}}{3}$. If $N_{step} > 0$, SF_k is decremented by one unit while $N_{step} < 0$ and $SF_k > SF_{min}$. Additionally, TP_k is reduced by 2 dBm while $N_{step} > 0$ and $TP_k > 2$ dBm. On the other hand, if $N_{step} < 0$, TP_k is incremented by 2 dBm while $N_{step} < 0$, and after each adjustment of TP_k , N_{step} is incremented by one unit [Marini et al., 2020].

2.1.3 Transmission Success Probability

In LoRaWAN networks, lower SFs enable higher packet transmission rates and shorter ToA, resulting in better throughput and lower collision probability. However, due to the lower receiver sensitivity associated with low SFs, the transmission range becomes more limited. On the other hand, higher SFs allow for broader coverage, but they lead to lower data rates, higher ToA, and increased collision rates [Wei et al., 2023].

Moreover, GWs are capable of receiving packets transmitted using any of the available SFs, which are quasi-orthogonal. This means that two signals using different SFs can be received simultaneously by the same GW with a high proba-

Algorithm 2: ADR Algorithm.

Input: ED to configure: ED_j , initial SF: SF_k , initial TP: TP_k , history of SNRs: S , number of last SNR values: N , SNR thresholds in dB: Γ

```

1  $SNR_{max} \leftarrow \text{GetMaxSnr}(ED_j, S, N)$ 
2  $SNR_{min} \leftarrow \text{MinSnrForSF}(\Gamma, SF_k)$ 
3  $SNR_{margin} \leftarrow SNR_{max} - SNR_{min} - 10$ 
4  $N_{step} \leftarrow \left\lfloor \frac{SNR_{margin}}{3} \right\rfloor$ 
5 if  $N_{step} > 0$  then
6   while  $N_{step} > 0$  and  $SF_k > SF_{min}$  do
7      $SF_k \leftarrow SF_k - 1$ 
8      $N_{step} \leftarrow N_{step} - 1$ 
9   while  $N_{step} > 0$  and  $TP_k > TP_{min}$  do
10     $TP_k \leftarrow TP_k - 2$  dBm
11     $N_{step} \leftarrow N_{step} - 1$ 
12 else
13   while  $N_{step} < 0$  and  $TP_k < TP_{max}$  do
14     $TP_k \leftarrow TP_k + 2$  dBm
15     $N_{step} \leftarrow N_{step} + 1$ 
16 return  $SF_k, TP_k$ 
```

bility of success, with negligible interference between the signals. Consequently, it is necessary to properly dimension the number of devices that can simultaneously use the same SF on the same frequency channel, in order to avoid degrading the intra-SF transmission capacity [Bouazizi et al., 2025].

Therefore, one of the main challenges in LoRaWAN networks is to define efficient SF allocation strategies capable of assigning an appropriate SF to each ED, while considering factors such as the ToA, the delay and reliability requirements of the running applications, and the total number of EDs in the network [Da Silva et al., 2024]. In this context, the probability of successful packet delivery for each SF can be estimated using Equation 6, as proposed in [Marini et al., 2020]:

$$p_{succ} = \left(1 - \frac{toa}{T}\right)^{2 \cdot (n-1)} \quad (6)$$

where toa is the ToA value, which indicates the time required to transmit a frame using a given SF, representing the duration a device occupies the channel in transmission mode; T is the interval between successive transmissions; the constant 2 refers to the expression $(2 \cdot ToA)$, which defines the minimum time interval that must be respected between consecutive transmissions to avoid collisions [Marini et al., 2020], since LoRaWAN employs ALOHA as its medium access protocol [LoRa Alliance, 2017]; and n corresponds to the number of devices simultaneously operating with a given SF.

2.2 Advanced Metering Infrastructure

The growing demand for power consumption, driven by factors such as population growth, industrial advancements, and increased use of electric vehicles, combined with the rise in renewable energy sources and distributed generators spread across the electrical system, makes it necessary to implement more efficient and proactive management of the EPS. Thus,

the deployment of AMI is a fundamental step in upgrading the EPS to a SG, as the data collected from the consumer side can be utilized by the utility company to enhance the quality of the service provided [Das and Bera, 2022].

The deployment of AMI allows utilities to take advantage of consumer data to improve the quality of the power supply, as well as to identify and resolve EPS malfunctions more quickly [Khan et al., 2021]. Its architecture is illustrated in Figure 2 and comprises SMs distributed across the Home Area Network (HAN), Building Area Network (BAN), and Industrial Area Network (IAN), which communicate with DAPs using a long-range communication technology such as LoRaWAN [Veloso et al., 2021]. DAPs, in turn, use a WAN connection to forward the data to control centers. The HAN covers residential areas, the BAN includes commercial and institutional buildings, and the IAN is responsible for industrial environments [Khan et al., 2022].



Figure 2. AMI System Architecture.

In the context of AMI, various applications coexist and can be classified into normal and critical traffic classes [Khan et al., 2022]. Normal traffic includes applications such as IMR and Billing. IMR transmits data related to electricity consumption, while Billing is associated with the collection, processing, and management of consumption data used to generate invoices and financial reports. In contrast, an example of a critical traffic application is PCC, which handles messages to execute load control actions [Khan et al., 2023].

These applications have QoS requirements primarily defined by the maximum delay, measured in seconds (s), the reliability rate, and the periodicity of message transmission in minutes (min), as shown in Table 2. Specifically, IMR transmits one packet every 5 to 60 min, with a maximum delay requirement of 60 s and a minimum reliability rate of 99%. Similarly, Billing typically sends one packet every 60 min and shares the same delay and reliability requirements as IMR. In contrast, PCC also transmits a message every 60 min but demands a maximum delivery delay of 1 s while maintaining a reliability rate of 99% [Khan et al., 2023].

Table 2. QoS Requirements of AMI Applications.

App	Delay (s)	Reliability (%)	Periodicity (min)
IMR	60	99–99.9	5–60
Billing	60	99–99.9	60
PCC	1	99	60

2.3 K-Means

K-Means is an algorithm used to form clusters from a dataset. This algorithm defines k centroids and a point is considered to be in a particular cluster if it is closer to that cluster centroid

than any other centroid. Thus, it can be described by the following steps according to [Gupta and Chandra, 2022]:

- Step 1: Select k random points from the dataset as the initial centroids of the clusters;
- Step 2: For each data point in the dataset, compute the distance between the point and each centroid. Assign each point to the cluster whose centroid is closest using a similarity measure, typically the Euclidean distance;
- Step 3: Recalculate the position of the centroids for each cluster. The new centroid is the mean of all points assigned to that cluster;
- Step 4: Repeat steps 2 and 3 until the centroids do not change significantly, or until a maximum number of iterations is reached. This indicates that the clusters have stabilized.

K-Means is mainly characterized by its simplicity of implementation, fast execution, and ability to handle large volumes of data [Yang and Hussain, 2023]. For this reason, it has been widely applied in the literature to position GWs in LoRaWAN networks [Loh et al., 2023; Correia et al., 2023], as well as to support communication infrastructure planning in AMI systems by determining the installation coordinates of DAPs to ensure proper application performance [Hsu et al., 2021; Lang et al., 2022]. In these use cases, K-Means applies the x and y coordinates of EDs and SMs to establish clusters and define the positions of GWs and DAPs, respectively, as the centroids of the clusters. Thus, the heights of GWs and DAPs are fixed (e.g., 30 m), as the model does not account for terrain elevation variations, which may reduce signal coverage.

3 Related Work

Several state-of-the-art proposals present solutions for SFA. For this reason, this section lists a set of works related to the scheme proposed in this paper, as shown in Table 3, and compares them based on the following criteria: (i) the name of the schemes defined in the references, which are used to identify the proposals; (ii) the main objectives these schemes aim to achieve related to improving the performance of the LoRaWAN technology; and (iii) the allocation strategy used to distribute SFs to the EDs.

The authors of [Farhad et al., 2020b] describe the ADR standard, which defines dynamic adjustments to the SF and TP values and transmits these adjustments through downlink messages to be received by the EDs. This scheme establishes the SF to be applied by an ED based on the current channel conditions, determined through SNR measurements extracted from a set of previously received packets at the GWs, which are forwarded to the NS. The adjustments to the SF are carried out with the goal of maintaining stable communication over the channel and, consequently, ensuring that the data transmitted by the EDs are continuously received by the GWs.

The paper developed by [Marini et al., 2020] proposes a scheme called CA-ADR, which aims to minimize the collision probability in LoRaWAN networks. To achieve this, the scheme determines the maximum number of devices that can use a given SF in order to ensure an effective transmission success rate on the channel, based on the network traffic

Table 3. Comparison of Related Work.

Reference	Scheme	Objective(s)	Allocation Strategy
Farhad <i>et al.</i> [2020b]	ADR	Maintain Stable Communication	Maximum SNR
Marini <i>et al.</i> [2020]	CA-ADR	Minimize Collisions and Ensure Reliability	SNR and Transmission Success Rate
Mao <i>et al.</i> [2021]	ADR+	Maintain Stable Communication and Improve Energy Efficiency	Average SNR
Farhad <i>et al.</i> [2020a]	M-ASFA	Reduce Losses and Retransmissions	Sensitivity and Motion Detection
Farhad <i>et al.</i> [2020b]	I-SFA	Reduce Losses	Sensitivity
Farhad <i>et al.</i> [2020c]	A-SFA	Reduce Interference	Sensitivity and Occurrence of Interference
Soto-Vergel <i>et al.</i> [2023]	I-SFA+ADR	Reduce Losses and Maintain Stable Communication	Sensitivity and Maximum SNR
Hazarika and Choudhury [2024]	iSFA	Increase Throughput and Reduce Energy Consumption	Clustering and Reinforcement Learning
This Paper	DR-SFA	Ensure Reliability and Maximum Delay, Reduce Costs	Sensitivity, Transmission Success Rate, and Maximum ToA

load and the ToA of each SF. Moreover, CA-ADR keeps the transmission power of the EDs fixed at 14 dBm, and the results demonstrate that this scheme is capable of maintaining an adequate packet delivery reliability for the tested applications under different link conditions.

The ADR+ scheme is described in [Mao *et al.*, 2021] and focuses on enhancing the operation of the standard ADR. To do this, ADR+ slightly modifies the NS-managed ADR by using the average SNR of the last N received packets instead of the maximum SNR. The results obtained from experiments with this scheme demonstrate that it increases the transmission consistency and energy efficiency of EDs under variable channel conditions. Thus, ADR+ shows improved performance in terms of data delivery reliability and reduced energy consumption when compared to typical ADR.

The authors of [Farhad *et al.*, 2020a] developed a scheme called Mobility-Aware Spreading Factor Allocation (M-ASFA), which aims to allocate the most suitable SF to EDs at each transmission by considering the signal strength received by GWs from the EDs. Initially, it assigns an appropriate SF to the EDs based on the GW sensitivity. Then, it dynamically reallocates a new SF to the EDs before each transmission if the device changes its position. This scheme is evaluated through simulations, and the results show that it improves communication reliability and reduces packet losses and retransmissions compared to the standard ADR, both in static and mobile scenarios.

The I-SFA scheme is also presented in [Farhad *et al.*, 2020b] and proposes a mechanism for allocating the SF of an ED based on the highest received power value among the GWs installed in the network for a previously transmitted packet, as described in Section 2. After determining the maximum received power, the scheme identifies the sensitivity range in which this value falls and then allocates an SF that has a lower probability of packet loss due to under sensitivity.

The scheme developed in [Farhad *et al.*, 2020c], referred to as Adaptive - Spreading Factor Allocation (A-SFA), enhances the operation of the I-SFA solution by adjusting the SF of an ED whenever a packet is lost due to interference. This scheme builds upon I-SFA, initially allocating the SFs based on the sensitivity range that matches the highest received power for

a packet transmitted by the ED, and subsequently performs dynamic adjustments by selecting a higher SF for packets lost due to interference. For instance, if an ED initially uses SF7 and one of its transmitted packets experiences interference, the scheme may increase the SF to a higher value in order to reduce losses due to interference in the channel.

The authors of [Soto-Vergel *et al.*, 2023] describe the I-SFA+ADR scheme, which combines the I-SFA and ADR mechanisms to adjust the SFs of the EDs. Initially, the scheme allocates SFs using I-SFA, and subsequently, as packets are transmitted through the network, dynamic adjustments are performed by ADR to maintain stable communication. The results of experiments with this scheme show that the use of I-SFA enables a more robust initial allocation, while the application of ADR allows the identification of channel degradation and reduces packet loss.

A machine learning-based scheme, called Intelligent Spreading Factor Allocation (iSFA), is proposed in [Hazarika and Choudhury, 2024] and adaptively selects the most suitable SF for EDs. This scheme jointly applies clustering and reinforcement learning techniques to optimize SF allocation in real-time networks, aiming to increase network throughput and reduce power consumption while ensuring application communication latency. Results obtained from a testbed demonstrate that iSFA improves network performance, extends battery life, and provides better adaptability to changing network conditions.

Finally, this paper introduces the DR-SFA scheme, which initially allocates SFs using the strategy defined by I-SFA and subsequently applies a transmission success rate formulation per SF, inspired by the mechanism defined in [Marini *et al.*, 2020], to reallocate a predetermined number of lower SFs to higher SFs. The objective is to ensure the required reliability and maximum communication delay for the running applications. Thus, DR-SFA balances the data traffic load across different SFs and assigns SFs to the EDs such that their ToA remains below the latency constraint specified by the applications, thereby reducing losses and minimizing the number of base stations needed to be deployed in the communication infrastructure.

4 Proposed Scheme

LoRaWAN was not designed to transmit data in real time or with delays of just a few seconds, and its performance is highly sensitive to the allocation of its operational parameters, especially the SF [Kumar *et al.*, 2023]. For applications with strict delay constraints, the ToA must be as low as possible, which leads to a preference for using lower SFs [Wei *et al.*, 2023]. However, the massive use of certain SFs degrades network performance [Magrin *et al.*, 2020]. For these reasons, this work proposes a SFA scheme that distributes the traffic load among the different SFs that ensure a ToA, ToA_{SF_j} , lower than the maximum delay allowed for the applications, T_{max} , as defined in Equation 7:

$$ToA_{SF_j} < T_{max} \quad (7)$$

The DR-SFA scheme applies the concept of received power sensitivity, also used by I-SFA, to define the initial distribution of SFs to the SMs. Subsequently, it reallocates higher SFs to a maximum number of devices that were previously assigned to use lower SFs. This SF change is guided by a formulation to guarantee a given success probability, p_{succ} , in packet delivery for each SF, with p_{succ} being obtained through Equation 6. Furthermore, DR-SFA is re-executed whenever the number of DAPs changes, resulting in a new SF allocation. Similarly, the allocation processes of the alternative schemes also produce a new SF distribution according to the number of DAPs.

DR-SFA determines the maximum number of devices that can operate with each SF to achieve the desired p_{succ} , denoted as $N_{SF_i}^{max}$, using a formulation that corresponds to an adaptation of the inverse of Equation 6 and is presented in Equation 8:

$$N_{SF_i}^{max} = \left\lceil \left(\frac{1}{2} \cdot \log_{\left(1 - \frac{ToA(SF_i)}{T}\right)}(p_{succ}) \right) + 1 \right\rceil \cdot 3 \quad (8)$$

where $ToA(SF_i)$ is the ToA for each SF_i , and 3 is the number of channels that the SMs can use to communicate with the DAPs in the European band [LoRa Alliance, 2017; More and Patel, 2023].

In order to detail the operation of the proposed scheme, Figure 3 and Algorithm 3 are presented and show that the I-SFA function, described in Algorithm 1, is executed and produces as output a quadruple of type τ , as illustrated in Step I of the flowchart and in lines 1 to 4 of the algorithm. These outputs are then added to V , the vector defined in Equation 9, which stores a number of records corresponding to the number of SMs in the network, N_{SMs} .

$$V = [\tau_1, \dots, \tau_{N_{SMs}}] \quad (9)$$

τ is described for Equation 10:

$$\tau = (SM_j, P_r^{max}, SF_k, DAP_i) \quad (10)$$

where SM_j is the SM identified by index j , P_r^{max} is the maximum received power for a packet from SM_j , SF_k is the SF to be assigned to SM_j , and DAP_i is the DAP identified by index i that receives the signal with power P_r^{max} .

The I-SFA function takes as input SM_j , the set of DAPs denoted by G , and S_{Rx} , which is the sensitivity vector per SF,

whose values are presented in the first column of Table 1. Using this function, DR-SFA allocates the initial SF for the set of SMs, M , which are assigned a TP of 14 dBm, and determines which DAP receives the strongest signal for each SM. Then, the scheme calculates the maximum number of SMs that can use each SF, $N_{SF_i}^{max}$, through the *CalcMaxNForSFs* function, which applies Equation 8 and takes as input the time interval between two successive transmissions in seconds, T ; the success probability required by the applications, p_{succ} ; and the ToA values for each SF, calculated using Equation 1, as presented in Step II of Figure 3 and on line 5 of Algorithm 3.

After $N_{SF_i}^{max}$ is determined, the scheme iterates over the set G , whose cardinality corresponds to the number of DAPs, N_{DAPs} . Then, the scheme randomly selects SMs to change their SF, ensuring that a set of constraints is satisfied, as shown in Step III of Figure 3 and in lines 6 to 16 of Algorithm 3. The first constraint is that the SF changes are performed using the set of SMs for which DAP_i is the DAP that received the strongest signal. That is, if there are 10 SMs, $[SM_1, \dots, SM_{10}]$, and 2 DAPs, $[DAP_1, DAP_2]$, and DAP_1 received packets with the highest signal strength from SM_1 and SM_{10} , then the changes are performed considering only these two SMs. In this way, the changes are executed for the SMs associated with a specific DAP, which are filtered from V .

The second constraint is that the changes are made by SF. First, a certain number of devices using SF7 are changed to SF8, then SF7 and SF8 are switched to SF9, and so on. Another constraint is that the function *ChangeSF* randomly selects a SM and performs the switch from a lower SF to a higher one only if the number of SMs assigned to the lower SF exceeds the maximum number of SMs allowed for that SF. That is, if $N_{SF_7}^{max} = 81$ and there are 82 SMs using SF7, then it is possible to change one SM to SF8 and $flag \leftarrow \text{True}$; otherwise, $flag \leftarrow \text{False}$. Moreover, a SM using a given SF, denoted as SF_i , can be reassigned to a higher SF, SF_j , if the transmission time toa_{SF_j} for SF_j is less than the maximum delay allowed for the applications executed by SM, T_{max} .

The proposed scheme also performs the SF swaps while the highest SF being assigned to other SMs has not yet reached its maximum allocation limit. For example, if DR-SFA is changing from SF7 to SF8, with $N_{SF_8}^{max} = 45$ and there are already 44 SMs configured with SF8, only one more SM can be assigned SF8 and $flag \leftarrow \text{True}$; otherwise, $flag \leftarrow \text{False}$. In this way, the scheme avoids overloading the higher SFs, which have longer ToA and are more susceptible to collisions [Farhad *et al.*, 2020c], unlike the alternatives schemes.

5 Methodology

This section presents the test scenarios, the parametrization of the LoRaWAN technology, and the evaluation metrics.

5.1 Simulation Setup

The evaluation of the proposed scheme is carried out through simulations using the Network Simulator 3 (NS-3) tool, ver-

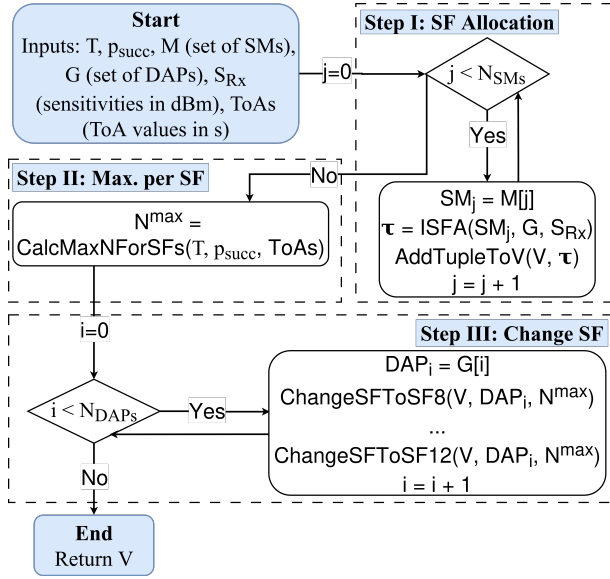


Figure 3. DR-SFA Scheme Flowchart.

Algorithm 3: DR-SFA Algorithm.

Input: interval in seconds: T , success probability: p_{succ} , set of SMs: M , set of DAPs: G , SF sensitivities in dBm: S_{Rx} , ToA for SFs in seconds: $ToAs$

```

1 for  $j \leftarrow 0$  to  $N_{SMs}$  do
2    $SM_j \leftarrow M[j]$ 
3    $\tau \leftarrow ISFA(SM_j, G, S)$ 
4    $AddTupleToV(V, \tau)$ 
5  $N^{max} \leftarrow CalcMaxNForSFs(T, p_{succ}, ToAs)$ 
6 for  $i \leftarrow 0$  to  $N_{DAPs}$  do
7    $DAP_i \leftarrow G[i]$ 
8    $flag \leftarrow True$ 
9   while  $flag == True$  do
10     $flag \leftarrow ChangeSF(V, DAP_i, N^{max}, 7, 8)$ 
11    ...
12     $flag \leftarrow True$ 
13    while  $flag == True$  do
14       $flag \leftarrow ChangeSF(V, DAP_i, N^{max}, 7, 12)$ 
15      ...
16       $flag \leftarrow ChangeSF(V, DAP_i, N^{max}, 11, 12)$ 
17 return  $V$ 
    
```

sion 3.43¹, complemented by the LoRaWAN module², which implements the SX1301 specification [Semtech, 2017]. The test scenarios simulate an urban square area of 7.5 km by 7.5 km (56.25 km²), with 200 to 1000 SMs distributed throughout this area. Each SM runs one IMR application, sending one packet every 12 minutes, and 50% of the SMs also run a PCC application, which sends one packet per hour. This results in a transmission interval, T , of 10 minutes, implying an average packet transmission rate of 1 pkt/10min.

Both applications transmit packets with a payload size of 51 B, a value commonly used in the literature for smart metering in LoRaWAN networks, as it allows the use of all

SFs [Veloso et al., 2021; Enriko et al., 2021]. The total simulation time is 24 hours, and each simulation is replicated 10 times with different random seeds to ensure the reliability of the results. These results are analyzed using a 95% confidence interval and the mean standard error. The LoRaWAN technology is configured to operate at a carrier frequency of 868 MHz, EU-868, with a bandwidth of 125 kHz. The DAPs are implemented as GWs, while the SMs are configured as EDs.

SMs are connected to the consumer energy panel, and the number of communication channels used is 3. The SMs operate with a TP ranging from 2 to 14 dBm, and the SF varies from 7 to 12, being allocated according to the schemes I-SFA, ADR, I-SFA+ADR, CA-ADR, and DR-SFA. The probability of success, p_{succ} , is set to 99%, which corresponds to the minimum reliability required by the applications. The maximum delay constraints are 1 s for PCC and 60 s for IMR. The number of DAPs tested starts at 1 and increases by one unit per simulation round, up to a maximum of 28, to ensure that p_{succ} is satisfied, forming a communication infrastructure represented in Figure 4.

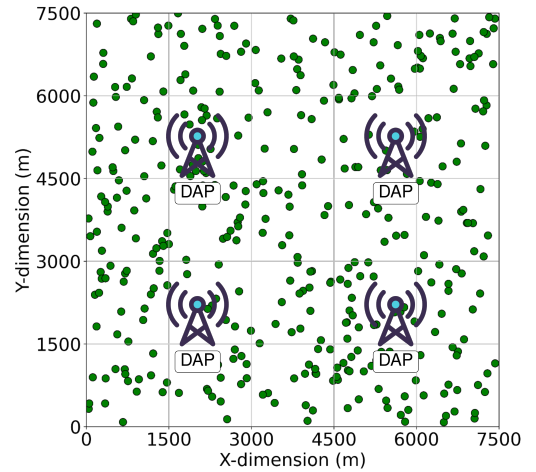


Figure 4. Example of an AMI system with 400 SMs.

SMs and DAPs are always placed at the same coordinates for all simulations in order to evaluate DR-SFA and the other schemes under identical conditions. To achieve this, the procedure illustrated in Figure 5 is used. It begins by executing the K-Means algorithm with three inputs: the number of clusters to generate, k ; the seed value for clustering, $seed$, which must remain the same across the tests of all SFA schemes to ensure that all use the same configurations; and the x and y coordinates of the SMs, denoted as $SMCoords$, which are fixed for all tests. These coordinates are then used to define the centroids, which correspond to the x and y positions of DAPs, represented as $DAPCoords$.

Additionally, the DAP height is set to 30 m, the SM height to 1.5 m, the applied CR is $\frac{4}{5}$, and the communication model follows the unconfirmed mode. Next, the Simulate step is executed to configure the scenario, run the simulation in NS-3 for each SFA scheme, $scheme$, compute the evaluation metrics, and store them in log files. One of these metrics is the PDR for the two tested applications, denoted as $PDRs$. If $PDRs \geq 99\%$ or $k == 28$, the procedure is finalized; otherwise, k is incremented by one and the procedure returns

¹<https://www.nsnam.org/releases/ns-3-43>
²<https://github.com/signetlabdei/lorawan>

to the execution of the K-Means algorithm.

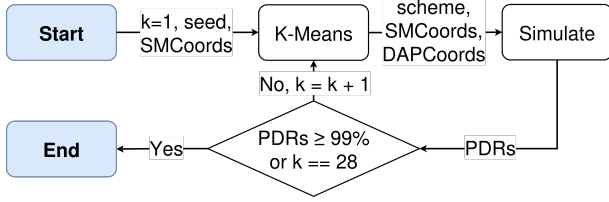


Figure 5. DAP Placement and Simulation Execution.

Furthermore, LoRaWAN is parameterized using the Log-Distance propagation loss model, with a path loss exponent of 3.76, to account for signal attenuation consistent with urban communication scenarios. The formulation describing the power loss calculation for this model is presented in Equation 11:

$$L(d) = L(d_0) + 10\gamma \log_{10} \left(\frac{d}{d_0} \right) + X_\sigma \quad (11)$$

where $L(d)$ represents the path loss in dB at a distance d from the transmitter, $L(d_0)$ is the path loss measured at a reference distance d_0 , γ is the path loss exponent, and X_σ represents shadowing, modeled as a normally distributed variable with a mean of zero and a standard deviation σ .

The Correlated Shadowing model is also used to add power loss due to shadowing and is described by a distance-dependent exponential function, $\rho_{i,j}$, which calculates the shadowing correlation experienced between two devices i and j , as presented in Equation 12:

$$\rho_{i,j}(d_{i,j}) = e^{-\frac{d_{i,j}}{d_c}} \quad (12)$$

where $d_{i,j}$ is the distance between nodes i and j and $d_c > 0$ is an adjustable parameter called decorrelation distance, representing the distance at which the shadowing correlation is below the threshold e^{-1} and therefore shadowing can be considered uncorrelated. Therefore, in order to apply a shadowing effect consistent with an urban scenario, the value of d_c is set to 110 m in the simulations. Given that all parameter configurations have been previously detailed, Table 4 summarizes the parameters used in this study along with their respective values.

Additionally, Table 5 presents the ToA values per SF for packets with a 51-byte payload, which corresponds to the data size transmitted by the tested applications. SF7 exhibits the lowest ToA, at 0.112896 s, while SF12 results in a ToA of 2.62963 s. This means that an SM using SF12 takes 23 times longer to complete the transmission of a packet on the channel than an SM using SF7. Furthermore, SF11 and SF12 have ToA values exceeding 1 s, making them unsuitable for SMs running PCC applications.

Thus, all these configurations are used to simulate an urban environment where smart metering applications transmit data to DAPs using LoRaWAN technology. For this reason, parameters such as simulation area, number of SMs, average transmission rate of the applications, and path loss coefficient are taken into account. Likewise, parameters such as bandwidth, number of frequency channels, CR, and applicable SF values are used to model typical LoRaWAN configurations

Table 4. Applied Parametrization.

Parameters	Values	Reference
Sim. Area	56.25 km ²	Farhad et al. [2020c]
SMs	200, 400, 600, 800, 1000	Neto et al. [2024]
IMR	100% of the SMs	Khan et al. [2022]
PCC	50% of the SMs	Khan et al. [2023]
λ_{IMR}	1 pkt/12min, 120 pkts/day	Khan et al. [2022]
λ_{PCC}	1 pkt/h, 24 pkts/day	Khan et al. [2023]
T	10 min	-
λ_{total}	1 pkt/10min, 144 pkts/day	-
Payload	51 B	Veloso et al. [2021]
Sim. Time	24 h (1 day)	Farhad et al. [2020b]
Frequency	868 MHz (EU-868)	Marini et al. [2022]
Bandwidth	125 kHz	Marini et al. [2022]
Channels	3	Farhad et al. [2020c]
TP	2 – 14 dBm	Veloso et al. [2021]
SF	7 – 12	Da Silva et al. [2024]
p_{succ}	99%	Khan et al. [2023]
Max. Delay	1 s (PCC), 60 s (IMR)	Khan et al. [2022] Khan et al. [2023]
DAPs	1 – 28	Da Silva et al. [2022]
DAP and SM Heights	30 m and 1.5 m	Farhad et al. [2020c]
CR	$\frac{4}{5}$	Da Silva et al. [2024]
Communication	Unconfirmed	Da Silva et al. [2024]
Propagation	Log Distance	Magrin et al. [2020]
γ	3.76	De Campos et al., [2024]
Shadowing	Correlated	Magrin et al. [2020]
d_c	110 m	Farhad et al. [2020c]

Table 5. ToA per SF for Packets with 51-Byte Payload.

SF	ToA (s)
SF7	0.112896
SF8	0.205312
SF9	0.369664
SF10	0.698368
SF11	1.47866
SF12	2.62963

in real-world deployments, contributing to the generation of meaningful performance evaluation results.

5.2 Evaluation Metrics

This section describes the evaluation metrics. The number of DAPs, N_{DAPs} , is used to assess the efficiency of the SFAs schemes [Lang et al., 2022], together with the metric S , which represents the average distance between SMs and DAPs, measuring the coverage range provided by DAPs in meters [Gallardo et al., 2021], and is calculated using Equation 13:

$$S = \frac{1}{N_{DAPs}} \cdot \sum_{m=1}^{N_{DAPs}} \left(\frac{1}{n_i} \cdot \sum_{j=1}^{n_i} s(\text{SM}_j, \text{DAP}_i) \right) \quad (13)$$

where n_i is the number of SMs that are closest to DAP_i , and $s(SM_j, DAP_i)$ represents the Euclidean distance [Gupta and Chandra, 2022] between SM_j and DAP_i .

A cost analysis considers the Capital Expenditure (CAPEX) in k€ , C_{apex} , includes the costs of purchasing, installing, and configuring the DAPs, as well as the expenses for setting up the transmission infrastructure needed for communication with the NS, and is described in Equation 14:

$$C_{apex} = 7.1 \cdot N_{DAPs} \quad (14)$$

where N_{DAPs} corresponds to the number of DAPs.

The PDR measures the reliability of communication [Jouhari et al., 2023] and is described by Equation 15:

$$PDR = \frac{N_{rec}}{N_{sent}} \quad (15)$$

where N_{sent} is the number of packets sent by the SMs, and N_{rec} is the number of packets successfully received with an adequate delay by the DAPs, as specified in Table 2.

SNR measures the communication quality [Da Silva et al., 2024], and the average SNR, \overline{snr} , is calculated by Equation 16:

$$\overline{snr} = \frac{1}{N_{Rec}} \sum_{i=1}^{N_{Rec}} snr_i \quad (16)$$

where snr_i corresponds to the SNR value for each successfully received packet.

The average delay, \overline{T} , measures the network ability to deliver data within the required time [Wei et al., 2023], and is calculated using Equation 17.

$$\overline{T} = \frac{1}{N_{Rec}} \cdot \left(\sum_{i=1}^{N_{Rec}} toa_i + p_i \right) \quad (17)$$

where toa_i is the ToA value and p_i is the propagation time of the i -th successfully received packet.

Packet loss occurrences are also evaluated, and these losses can be due to several causes, as established in [Farhad et al., 2020c]: (i) interference, losses caused by collisions; (ii) under sensitivity, when packets are received with a power level below the minimum required for correct reception for the corresponding SF, as shown in Table 1; (iii) DAP saturation, which occurs when the DAP is overloaded and can no longer receive uplink packets; (iv) DAP in transmission mode, when the DAP is sending a downlink packet, such as a dynamic SF adjustment message generated by ADR, and incoming uplink packets are discarded; and (v) expired messages, when packets are received by DAPs with a delay longer than the application requirement. Furthermore, the packet loss analysis considers that the same packet may be affected by different types of loss, or even the same type of loss at multiple DAPs, since a given packet can be received by more than one DAP, or even by all DAPs in the LoRaWAN network [Magrin et al., 2020].

The metric $\eta(SF_i)$ represents the percentage of SMs using a given SF [Loubany et al., 2023] and is calculated by Equation 18:

$$\eta(SF_i) = \frac{N_{SF_i}}{N_{SMs}}, \quad \forall i \in \{7, 8, 9, 10, 11, 12\} \quad (18)$$

where N_{SF_i} is the number of SMs operating with SF_i .

The metric $\psi(TP_i)$ represents the percentage of SMs using a given TP [Al-Gumaei et al., 2021] and is calculated by Equation 19:

$$\psi(TP_i) = \frac{N_{TP_i}}{N_{SMs}}, \quad \forall i \in \{2, 4, 6, 8, 10, 12, 14\} \quad (19)$$

where N_{TP_i} is the number of SMs that operate with TP_i .

6 Results and Discussion

This section presents the evaluation results of DR-SFA and the alternative schemes, based on simulations conducted according to the setup presented in Section 5.

The number of DAPs required by the schemes is shown in Figure 6, and it demonstrates that DR-SFA employs fewer DAPs to achieve the minimum reliability rate of 99% for packets successfully delivered within the appropriate time. For the scenarios with 200 and 400 SMs, both DR-SFA and I-SFA utilize 2 and 3 DAPs, respectively, while the other schemes require more DAPs. In the scenario with 200 SMs, DR-SFA reduces the number of DAPs by 80% compared to I-SFA+ADR, by 86.67% compared to CA-ADR, and by 92.86% compared to ADR. Additionally, DR-SFA requires 4 DAPs for the scenario with 1000 SMs, achieving reductions of 20% and 55.56% compared to I-SFA and I-SFA+ADR, respectively, and 85.71% with respect to both CA-ADR and ADR.

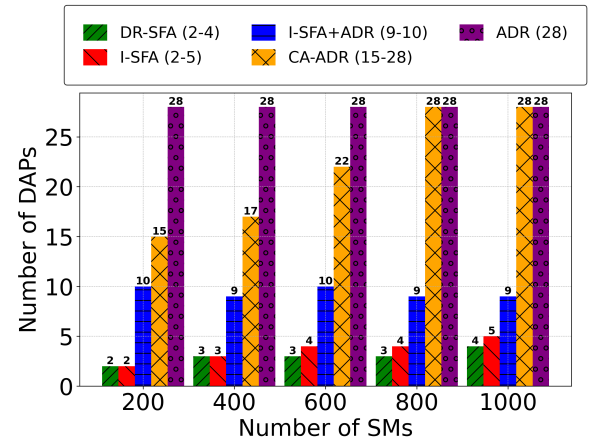


Figure 6. Number of DAPs for SFA Schemes.

The average communication distances achieved by the evaluated schemes are presented in Figure 7, and it highlights that DR-SFA is capable of allocating SFs in a way that increases the distance between SMs and DAPs, thereby achieving broader signal coverage with fewer DAPs compared to the alternative schemes, especially when compared to ADR. For the scenario with 200 SMs, DR-SFA achieves the same average distance as I-SFA, 2197.56 m, which is 5.29 times greater than the signal range of ADR. On the other hand, for

the scenario with 600 SMs, DR-SFA achieves an average distance of 1732.68 m, the highest among all schemes. Finally, for the scenario with 1000 SMs, DR-SFA again achieves the longest average distance, 1438.47 m, which corresponds to 2.83 times the range of ADR.

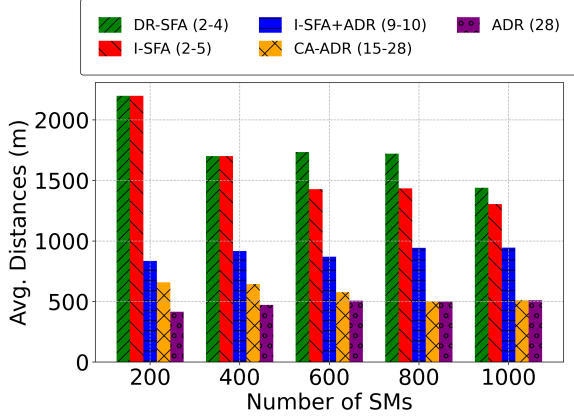


Figure 7. Average Distances for SFA Schemes.

Figure 8 presents the CAPEX values obtained by the SFA schemes. DR-SFA presents the lowest costs across all test scenarios, while ADR consistently incurs the highest costs. In contrast, although CA-ADR applies a SF distribution based on success probability, it employs more DAPs than I-SFA and I-SFA+ADR, leading to higher costs than those schemes and DR-SFA as well. For the scenario with 200 SMs, DR-SFA incurs a cost of 14.20 k€, representing a reduction of 184.60 k€ compared to ADR. On the other hand, in the scenario with 1000 SMs, it reduces the CAPEX by 170.40 k€ compared to both CA-ADR and ADR.

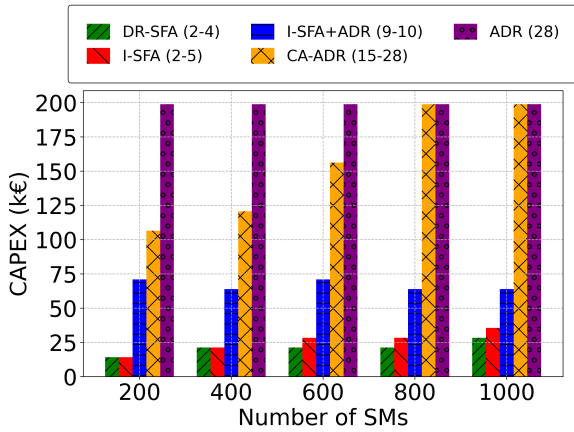


Figure 8. CAPEX for SFA Schemes.

Figure 9 shows the PDR values for both tested applications and highlights the potential of DR-SFA, which, despite using the lowest number of DAPs, outperforms ADR, as the latter is unable to ensure 99% reliability even with 28 DAPs. DR-SFA also achieves higher PDR than I-SFA in the test scenarios, except for the one with 800 SMs, and performs similarly to I-SFA+ADR in the scenarios with 400, 600, and 1000 SMs, with overlapping confidence intervals. Additionally, compared to CA-ADR, DR-SFA exhibits slightly lower PDR, but the difference is at most 0.3%. For the scenario with the largest number of meters, 1000, DR-SFA reaches

an average PDR of 99.49% (± 0.02), while I-SFA+ADR achieves 99.45%, and CA-ADR reaches 99.79%. Ultimately, CA-ADR demonstrates superior packet delivery performance in comparison to ADR.

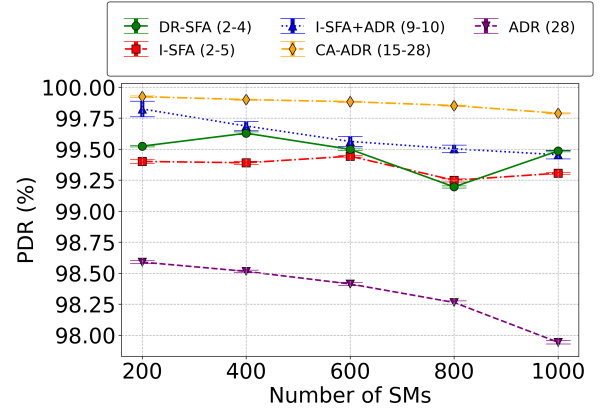


Figure 9. PDR for SFA Schemes.

Figure 10 presents the PDR values obtained by the schemes for the IMR application, which has a delay constraint of 60 s, as shown in Table 2. The results indicate that DR-SFA is able to deliver more packets than I-SFA. Moreover, in the scenario with 1000 SMs and 4 DAPs, DR-SFA achieves a PDR of 99.49% (± 0.02), which is higher than the values obtained by I-SFA and ADR, even though these schemes use more DAPs. Additionally, for the same scenario, I-SFA+ADR and DR-SFA present overlapping confidence intervals. Therefore, this metric demonstrates that the scheme proposed in this paper satisfies the QoS requirements of the IMR application with fewer DAPs, without compromising data delivery reliability.

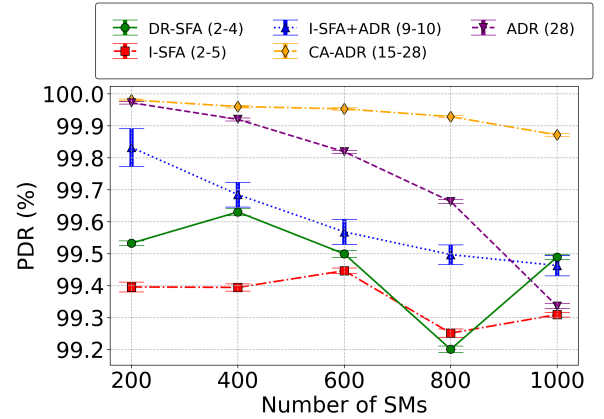


Figure 10. PDR for the IMR Application.

PDR for the PCC application, which has strict requirements of a maximum delay of 1 s and a minimum reliability rate of 99%, is presented in Figure 11. As shown, ADR does not meet the delay constraint and achieves a PDR of approximately 84% across all test scenarios. Regarding the DR-SFA, I-SFA, and I-SFA+ADR schemes, all ensure proper operation of the application and exhibit similar performance, with the highest value achieved by DR-SFA being 99.61% (± 0.07) for 400 SMs, indicating that limiting SF allocation based on the constraint defined in Equation 7 is effective. In contrast, CA-ADR shows a performance comparable to the other schemes for scenarios with 200 to 800 SMs, but does not meet

the requirements for 1000 SMs, achieving an average PDR of 98.97%.

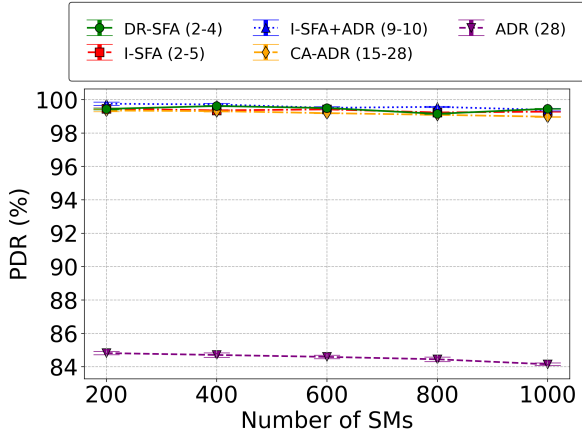


Figure 11. PDR for the PCC Application.

Figure 12 shows the SNR values obtained by the schemes and demonstrates that DR-SFA achieves better SNR performance, despite allocating a greater number of higher SFs compared to the other schemes. These findings support the assessment that the SF distribution strategy applied by the proposed scheme is promising, as it reduces power loss, mitigates noise, and more efficiently balances the traffic load across SFs, reaching -16.98 dB (± 0.05) for 1000 SMs. Furthermore, the results show that I-SFA is capable of transmitting signals with performance close to that achieved by DR-SFA.

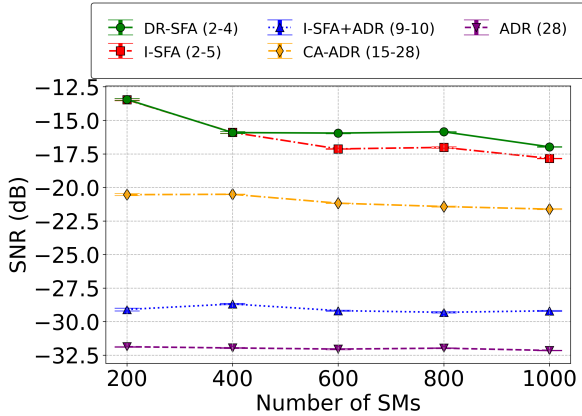


Figure 12. SNR for SFA Schemes.

The average delay values for both applications are shown in Figure 13, highlighting that I-SFA and I-SFA+ADR achieve the lowest delays due to employing a higher proportion of lower SFs compared to the other schemes, while ADR results in the highest average delay. In contrast, DR-SFA presents a maximum delay of 219.67 ms (± 4.32) for the scenario with 600 SMs and 3 DAPs, indicating that the SF allocation strategy of this scheme is capable of meeting the maximum delay requirement imposed by the tested applications. Finally, CA-ADR shows performance similar to DR-SFA in the scenarios with 800 and 1000 SMs, although it relies on a larger number of DAPs.

The delay values for the PCC application are shown in Figure 14. This metric is analyzed due to its more stringent maximum delivery delay requirement, limited to 1 s, as pre-

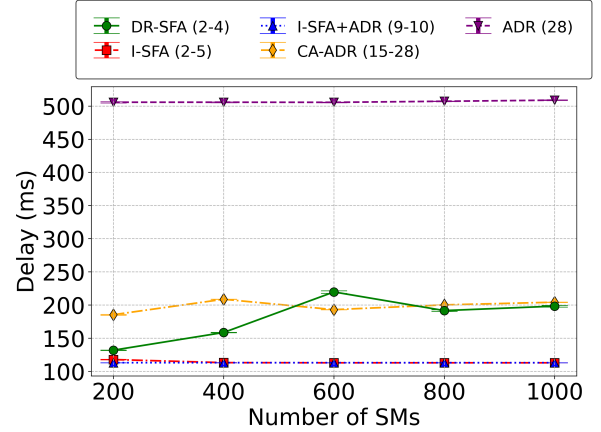


Figure 13. Delay for SFA Schemes.

sented in Table 2. Delays are generally higher for DR-SFA, except in the scenarios with 200 and 400 SMs, where CA-ADR applies more higher SFs and consequently has a longer average delay. Furthermore, the highest delay observed for DR-SFA is 215.03 ms (± 2.99) in the scenario with 600 SMs, which is significantly lower than the 1 s requirement of PCC. Finally, ADR presents a PDR of 84%, as shown in Figure 11, and a delay similar to I-SFA and I-SFA+ADR due to the fact that the packets it receives are sent using low SFs.

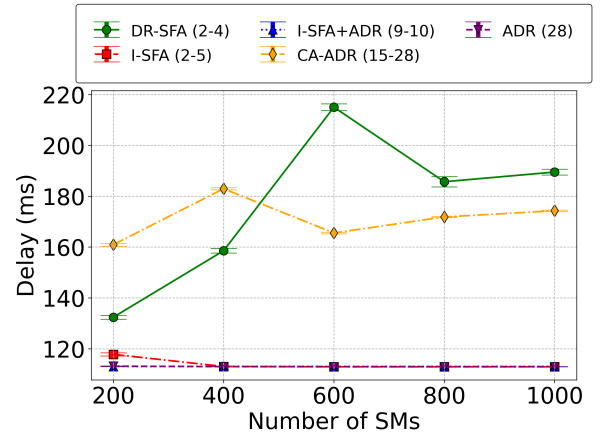


Figure 14. Delay for the PCC Application.

The number of packets lost due to interference and under sensitivity by the DAPs for the SFA schemes are presented in Figures 15–16, respectively. These two types of losses are analyzed as they represent the main causes of packet loss across all the evaluated schemes, since losses caused by the DAP being in transmission mode occur only for ADR and CA-ADR and have a significantly lower number of occurrences compared to interference and under sensitivity. Similarly, losses due to expired packets do not occur for DR-SFA and I-SFA, and their frequency is low for the other schemes, as is the case for losses due to saturation of the DAPs reception capacity.

Figure 15 shows that DR-SFA outperforms I-SFA, ADR, and CA-ADR, but loses more packets due to interference than I-SFA+ADR. This occurs because I-SFA+ADR is more susceptible to under sensitivity, meaning that more packets are received with power levels below the minimum reception threshold defined in Table 1, and thus cannot be properly demodulated for subsequent interference checking. Addi-

tionally, the highest number of such losses for DR-SFA is observed in the scenario with 1000 SMs, totaling 2234 lost packets (± 36), which corresponds to a reduction of 31.04%, 50.43%, and 83.84% compared to I-SFA, CA-ADR, and ADR, respectively.

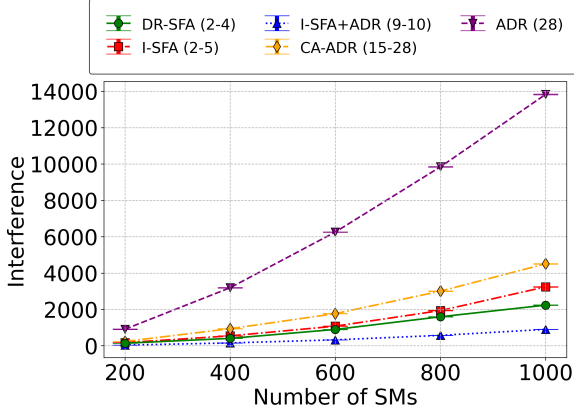


Figure 15. Losses due to Interference for SFA Schemes.

Figure 16 presents the number of packets lost due to under sensitivity, and DR-SFA consistently loses fewer packets than the alternative schemes in all scenarios, achieving a reduction of 15.82%, 29.46%, 49.7%, and 53.96% for 1000 SMs, compared to I-SFA, CA-ADR, ADR, and I-SFA+ADR, respectively. ADR and I-SFA+ADR suffer more losses of this type because the allocation of SFs and TPs, which is performed dynamically as new packets are received by the DAPs, tends to prioritize the reduction of SFs and TPs. As a result, many transmitted packets reach multiple DAPs with power levels below the minimum reception threshold defined for each SF.

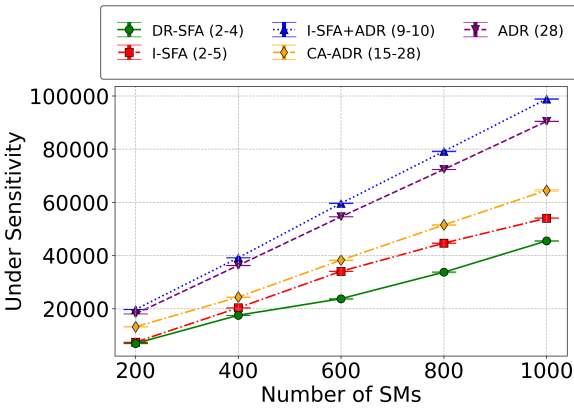


Figure 16. Losses due to Under Sensitivity for SFA Schemes.

Figure 17 shows the final SF distribution for the scenario with 600 SMs. Based on the results, DR-SFA employs SF7 to SF11, with SMs running exclusively the IMR application being configured with SF11. In this scheme, 55.9% of the SMs use SF7, while only 0.6% operate with SF11. In contrast, I-SFA and I-SFA+ADR apply only SF7, since their estimation of the best SF considers the highest received power based on path loss and shadowing, disregarding interference losses. As the number of DAPs increases, the received signal strength also tends to increase, further reinforcing the selection of SF7. On the other hand, CA-ADR uses the full range of SFs, assigning SF7 to 51.65% of the SMs and SF12 to 1.77%.

Meanwhile, ADR allocates SF7 to all SMs, as it operates with 28 DAPs.

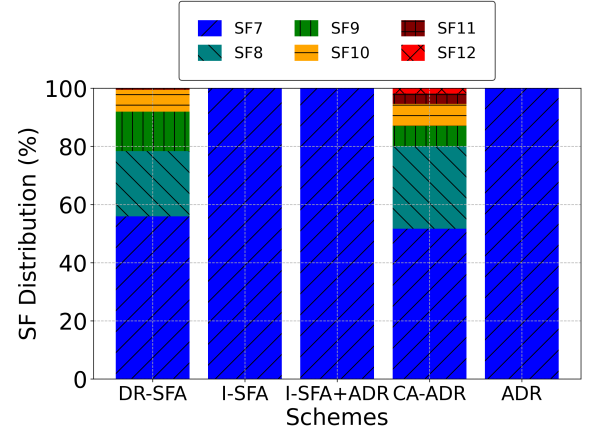


Figure 17. Final SF Distribution for 600 SMs.

The SF distribution for the scenario with 1000 SMs is presented in Figure 18. The DR-SFA scheme allocates SFs from SF7 to SF11, restricting the use of SF11 to SMs that exclusively run the IMR application. Additionally, DR-SFA distributes the SFs so as to alleviate traffic on the lower SFs, thereby reducing interference levels in these channels. In contrast, I-SFA, I-SFA+ADR, and ADR assign SF7 to all SMs, overloading this SF and increasing the likelihood of channel interference. Meanwhile, CA-ADR employs the full range of SFs despite the maximum allowed delay for PCC being limited to 1 s, with 49.5% of the SMs operating on SF7 and 1.67% on SF12.

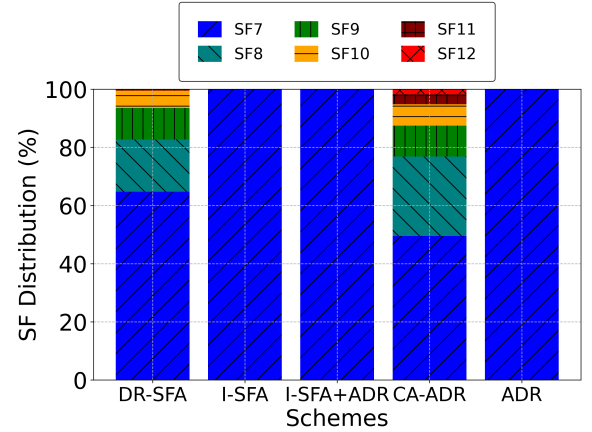


Figure 18. Final SF Distribution for 1000 SMs.

The TP distribution for the scenario with 1000 SMs is presented in Figure 19, focusing on the scenario with the highest SMs density per area, as the other scenarios exhibit a similar distribution pattern. The DR-SFA, I-SFA, and CA-ADR schemes allocate only a TP of 14 dBm to the SMs, which helps to reduce the probability of under sensitivity losses at the DAPs. In contrast, I-SFA+ADR distributes TP values between 2 and 14 dBm, most frequently assigning 2 dBm to the SMs, which increases the likelihood of power loss over the channel and results in a higher rate of packet losses due to under sensitivity. Meanwhile, ADR applies only SF7 and SF8, with 99.25% of the SMs operating with SF7, which compromises transmission reliability.

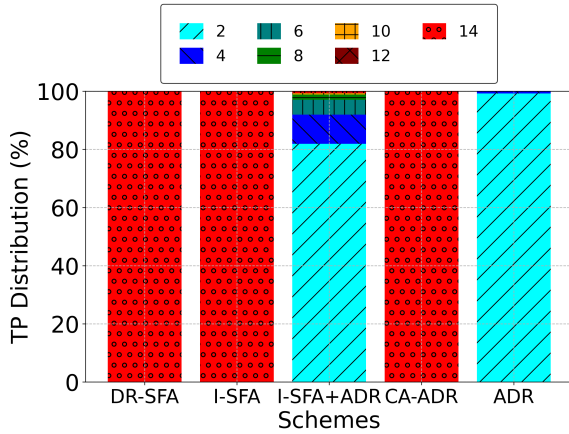


Figure 19. Final TP Distribution for 1000 SMs.

All evaluated performance metrics demonstrate that DR-SFA adopts a promising SF allocation strategy. It effectively balances the use of lower SFs, which offer shorter ToA, to meet the latency requirements of the IMR application, while also leveraging higher SFs to reduce the traffic load on the lower ones. This strategy contributes to a more stable utilization of the LoRaWAN technology, as evidenced by the results obtained for simulated scenarios with varying numbers of SMs. In contrast, the I-SFA scheme achieves high average PDR values across the test scenarios but requires a larger number of DAPs to ensure the minimum 99% packet delivery reliability.

Another analysis that reinforces the applicability of DR-SFA is the fact that, even employing fewer DAPs, receiving packets from SMs located farther from the DAPs, and utilizing a higher proportion of elevated SFs, the signal quality – measured through the SNR metric – is superior to that obtained by alternative solutions. Furthermore, DR-SFA reduces interference-related losses when compared to I-SFA, CA-ADR, and ADR. Although it experiences a slightly higher number of interfered packets than I-SFA+ADR, when the number of packets lost due to both interference and under sensitivity are combined, DR-SFA yields a significantly lower total packet loss.

This indicates that the dynamic allocation of SF and TP performed by I-SFA+ADR is not sufficiently robust to adapt to channel fluctuations, whereas DR-SFA is able to demodulate more packets transmitted at lower power levels and from more distant devices. In contrast, I-SFA+ADR shows a reduced capacity to receive such packets, which are discarded before the DAP can even verify whether they have suffered interference. Moreover, the allocation of the maximum TP value (14 dBm) to SMs by DR-SFA reduces losses due to under sensitivity and does not significantly impact meter efficiency, as the devices are connected to the consumer power grid. Ultimately, when compared to CA-ADR, DR-SFA operates more efficiently, which demonstrates that the maximum SF allocation strategy is effective.

Additionally, the delay-related results indicate that the communication latency achieved by DR-SFA is higher than in some alternative schemes, since it employs a greater proportion of higher SFs. Nevertheless, DR-SFA can still meet the maximum delay requirements for both the IMR and PCC applications. For PCC, the highest average delay observed

remains below 220 ms, whereas the application allows a maximum delivery delay of 1 s (1000 ms), as shown in Table 2. Therefore, the proposed scheme successfully applies higher SFs while ensuring that a given SF is only assigned if all applications executed by a given SM have delay constraints greater than the ToA of the respective SF.

Finally, the SFA schemes were tested in scenarios with static SMs, which is the main operating mode of these devices. It was also assumed that all nodes are active and transmit during the simulations, indicating that further tests considering mobility and more complex scenarios would be beneficial. Moreover, adjusting the TP values of the meters would be relevant for the evolution of the allocation scheme, aiming to evaluate the impact of this parameter on the performance of smart metering applications.

7 Conclusion

This paper proposes a scheme called DR-SFA, which aims to allocate the maximum number of SMs to each SF while ensuring the minimum required Packet Delivery Reliability and delay constraints of the Interval Meter Reading and Power-Control Command applications. The validation of DR-SFA is performed through simulations with 200 to 1000 SMs distributed over an area of 56.25 km², and the scheme is compared with I-SFA, ADR, I-SFA+ADR, and CA-ADR.

The results show that DR-SFA is promising, as it reduces the number of DAPs by up to 92.86%, lowers CAPEX by up to 184.60 k€, and provides a signal coverage of approximately 2197.56 m, ensuring packet reception within the appropriate latency. Furthermore, for the scenario with 1000 SMs and 4 DAPs, DR-SFA achieves a PDR of 99.49%, while also decreasing packet loss due to interference by 83.84% compared to ADR, and packet loss due to under sensitivity by 53.96% compared to I-SFA+ADR. Regarding delay, the maximum value obtained by DR-SFA is below 220 ms, and all these analyses demonstrate the efficiency of the proposed scheme.

The results also demonstrate the applicability of LoRaWAN technology for transmitting data from smart metering. Despite this IoT technology operating with a 125 kHz bandwidth and employing ALOHA as its medium access mechanism, it is still able to meet the requirements of the tested applications. Furthermore, LoRaWAN uses an unlicensed frequency band, offers low deployment and maintenance costs, enables the construction of private infrastructure, and is well suited for transmitting small volumes of data, such as those generated by the smart metering applications considered in this paper.

In contrast, solutions such as 5G and NarrowBand IoT (NB-IoT) are technologies that offer better performance than LoRaWAN. However, these more robust solutions operate on licensed frequency bands and require a data plan contracted with mobile network operators in order to enable the execution of smart metering applications [Al-Sammak et al., 2025]. Therefore, adopting 5G or NB-IoT would increase the cost of communication infrastructure for the electrical utility and would not allow the deployment of a simpler private network dedicated to operating the AMI system.

Finally, DR-SFA should be enhanced to define the min-

imum TP values that can be allocated to SMs, while still maintaining the required reliability and improving the energy efficiency of the SMs. Moreover, studies should be conducted to propose strategies for reducing network collisions, minimizing packet losses caused by interference, and testing the scheme in scenarios with mobile devices. Additionally, extending the placement model based on clustering to incorporate terrain altitude is an important direction for future work.

Acknowledgements

Acknowledgements to the support of Instituto Federal do Maranhão (IFMA) and Fundação de Amparo à Pesquisa do Maranhão (FAPEMA).

Funding

This research was funded by FAPEMA via Grant No. 004542/2023.

Authors' Contributions

TARS contributed to the conception of this study and wrote the main manuscript. TARS, GASN and LHOM performed the experiments. TARS, FJVS, and PFFA handled the preparation and review of all figures and tables. JVRJ contributed to the final revision of the manuscript. All authors read and approved the final manuscript.

Competing interests

The authors declare that they have no competing interests.

Availability of data and materials

This paper did not utilize datasets. All evaluations were performed in an experimental simulation environment.

References

- Abd Elkarim, S. I., Elsherbini, M. M., Mohammed, O., Khan, W. U., Waqar, O., and ElHalawany, B. M. (2022). Deep learning based joint collision detection and spreading factor allocation in lorawan. In *2022 IEEE 42nd International Conference on Distributed Computing Systems Workshops (ICDCSW)*, pages 187–192. IEEE. DOI: 10.1109/ICDCSW56584.2022.00043.
- Al-Gumaei, Y. A., Aslam, N., Chen, X., Raza, M., and Ansari, R. I. (2021). Optimizing power allocation in lorawan iot applications. *IEEE Internet of Things Journal*, 9(5):3429–3442. DOI: 10.1109/JIOT.2021.3098477.
- Al-Sammak, K. A., Al-Gburi, S. H., Marghescu, C., Drăgulescu, A. M., Suci, G., and Abdulqader, A. G. (2024). A comprehensive assessment of lorawan and nb-iot performance metrics under varied payload data sizes. In *2024 16th International Conference on Electronics, Computers and Artificial Intelligence (ECAI)*, pages 1–5. DOI: 10.1109/ECAI61503.2024.10607481.
- Al-Sammak, K. A., Al-Gburi, S. H., Marghescu, I., Drăgulescu, A.-M. C., Marghescu, C., Martian, A., Al-Sammak, N. A. H., Suci, G., and Alheeti, K. M. A. (2025). Optimizing iot energy efficiency: Real-time adaptive algorithms for smart meters with lorawan and nb-iot. *Energies*, 18(4):987. DOI: 10.3390/en18040987.
- Alumfareh, M. F., Humayun, M., Ahmad, Z., and Khan, A. (2024). An intelligent lorawan-based iot device for monitoring and control solutions in smart farming through anomaly detection integrated with unsupervised machine learning. *IEEE Access*. DOI: 10.1109/ACCESS.2024.3450587.
- Bouazizi, Y., Benkhelifa, F., ElSawy, H., and McCann, J. A. (2025). Sf-adaptive duty-cycled lora networks: Scalability, reliability, and latency tradeoffs. *IEEE Transactions on Communications*, 73(2):1042–1057. DOI: 10.1109/TCOMM.2024.3450586.
- Correia, F. P., Silva, S. R. d., Carvalho, F. B. S. d., Alencar, M. S. d., Assis, K. D. R., and Bacurau, R. M. (2023). Lorawan gateway placement in smart agriculture: An analysis of clustering algorithms and performance metrics. *Energies*, 16(5):1–21. DOI: 10.3390/en16052356.
- Da Silva, C. N., de Abreu, P. F. F., da Silveira, J. D. F., and dos R, J. V. (2022). Estimating the number of gateways through placement strategies in a lorawan network. In *2022 XII Brazilian Symposium on Computing Systems Engineering (SBESC)*, pages 1–6. DOI: 10.1109/SBESC56799.2022.9964620.
- Da Silva, T. A. R., Sarmiento Neto, G. A., Abreu, P. F. F., Veloso, A. F. D. S., Mendes, L. H. d. O., and Dos Reis, J. V. (2024). A novel data aggregation point placement method for smart metering service using lorawan technology. In *2024 11th International Conference on Future Internet of Things and Cloud (FiCloud)*, pages 55–62. DOI: 10.1109/FiCloud62933.2024.00017.
- Das, R. and Bera, J. N. (2022). Quality of service improvement in neighborhood area networking for ami with zigbee-based tunable clustered scale-free topology and rpl routing. *IEEE Transactions on Smart Grid*, 14(1):453–463. DOI: 10.1109/TSG.2022.3191358.
- Enriko, I. K. A., Abidin, A. Z., and Noor, A. S. (2021). Design and implementation of lorawan-based smart meter system for rural electrification. In *2021 International Conference on Green Energy, Computing and Sustainable Technology (GECOST)*, pages 1–5. IEEE. DOI: 10.1109/GECOST52368.2021.9538704.
- Farhad, A., Kim, D.-H., Kim, B.-H., Mohammed, A. F. Y., and Pyun, J.-Y. (2020a). Mobility-aware resource assignment to iot applications in long-range wide area networks. *IEEE Access*, 8:186111–186124. DOI: 10.1109/ACCESS.2020.3029575.
- Farhad, A., Kim, D.-H., Subedi, S., and Pyun, J.-Y. (2020b). Enhanced lorawan adaptive data rate for mobile internet of things devices. *Sensors*, 20(22):6466. DOI: 10.3390/s20226466.
- Farhad, S., Lodhi, M. A., Khan, W. U., and Masood, F. (2020c). An adaptive and lightweight spreading factor assignment scheme for lorawan networks. In *2020 14th International Conference on Open Source Systems and Technologies (ICOSST)*, pages 1–6. IEEE. DOI:

- 10.1109/ICOSTS51357.2020.9333065.
- Gallardo, J. L., Ahmed, M. A., and Jara, N. (2021). Clustering algorithm-based network planning for advanced metering infrastructure in smart grid. *IEEE Access*, 9:48992–49006. DOI: 10.1109/ACCESS.2021.3068752.
- Gupta, M. K. and Chandra, P. (2022). Effects of similarity/distance metrics on k-means algorithm with respect to its applications in iot and multimedia: a review. *Multimedia Tools and Applications*, 81(26):37007–37032. DOI: 10.1007/s11042-021-11255-7.
- Hazarika, A. and Choudhury, N. (2024). isfa: Intelligent sf allocation approach for lora-based mobile and static end devices. In *2024 IEEE Wireless Communications and Networking Conference (WCNC)*, pages 1–6. IEEE. DOI: 10.1109/WCNC57260.2024.10570655.
- Hsu, H.-C., Zhuang, S.-R., and Huang, Y.-F. (2021). Cost-effective data aggregation method for smart grid. *Electronics*, 10(23):1–13. DOI: 10.3390/electronics10232911.
- Jouhari, M., Saeed, N., Alouini, M.-S., and Amhoud, E. M. (2023). A survey on scalable lorawan for massive iot: Recent advances, potentials, and challenges. *IEEE Communications Surveys & Tutorials*, 25(3):1841–1876. DOI: 10.1109/COMST.2023.3274934.
- Júnior, J. A. d. O., de Camargo, E. T., and Seiji Oyamada, M. (2023). Data compression in lora networks: A compromise between performance and energy consumption. *Journal of Internet Services and Applications*, 14(1):95–106. DOI: 10.5753/jisa.2023.3000.
- Khan, A., Shirazi, S. H., Adeel, M., Assam, M., Ghadi, Y. Y., Mohamed, H. G., and Xie, Y. (2023). A qos-aware data aggregation strategy for resource constrained iot-enabled ami network in smart grid. *IEEE Access*. DOI: 10.1109/ACCESS.2023.3312552.
- Khan, A., Umar, A. I., Munir, A., Shirazi, S. H., Khan, M. A., and Adnan, M. (2021). A qos-aware machine learning-based framework for ami applications in smart grids. *Energies*, 14(23):8171. DOI: 10.3390/en14238171.
- Khan, A., Umar, A. I., Shirazi, S. H., Ishaq, W., Shah, M., Assam, M., and Mohamed, A. (2022). Qos-aware cost minimization strategy for ami applications in smart grid using cloud computing. *Sensors*, 22(13):4969. DOI: 10.3390/s22134969.
- Kumar, B. S., Ramalingam, S., Divya, V., Amruthavarshini, S., and Dhivyashree, S. (2023). Lora-iot based industrial automation motor speed control monitoring system. In *2023 International Conference on Intelligent Data Communication Technologies and Internet of Things (IDCIoT)*, pages 11–15. IEEE. DOI: 10.1109/IDCIoT56793.2023.10053525.
- Lang, A., Wang, Y., Feng, C., Stai, E., and Hug, G. (2022). Data aggregation point placement for smart meters in the smart grid. *IEEE Transactions on Smart Grid*, 13(1):541–554. DOI: 10.1109/TSG.2021.3119904.
- Loh, F., Baur, C., Geißler, S., ElBakoury, H., and Hoßfeld, T. (2023). Collision and energy efficiency assessment of lorawans with cluster-based gateway placement. In *2023 IEEE International Conference on Communications Workshops (ICC Workshops)*, pages 391–396. IEEE. DOI: 10.1109/ICCWorkshops...556. DOI: 10.1109/icc-workshops57953.2023.10283556.
- LoRa Alliance, I. (2017). Lorawan 1.1 specification. <https://resources.lora-alliance.org/technical-specifications/lorawan-specification-v1-1>. Accessed: 2025-07-09.
- Loubany, A., Lahoud, S., Samhat, A. E., and El Helou, M. (2023). Throughput improvement for lorawan networks considering iot applications priority. In *2023 6th Conference on Cloud and Internet of Things (CIoT)*, pages 206–210. IEEE. DOI: 10.1109/CIoT57267.2023.10084887.
- Magrin, D., Capuzzo, M., and Zanella, A. (2020). A through study of lorawan performance under different parameter settings. *IEEE Internet of Things Journal*, 7(1):116–127. DOI: 10.1109/JIOT.2019.2946487.
- Mao, W., Zhao, Z., Chang, Z., Min, G., and Gao, W. (2021). Energy-efficient industrial internet of things: Overview and open issues. *IEEE transactions on industrial informatics*, 17(11):7225–7237. DOI: 10.1109/TII.2021.3067026.
- Marini, R., Cerroni, W., and Buratti, C. (2020). A novel collision-aware adaptive data rate algorithm for lorawan networks. *IEEE Internet of Things Journal*, 8(4):2670–2680. DOI: 10.1109/JIOT.2020.3020189.
- Marini, R., Mikhaylov, K., Pasolini, G., and Buratti, C. (2022). Low-power wide-area networks: Comparison of lorawan and nb-iot performance. *IEEE Internet of Things Journal*, 9(21):21051–21063. DOI: 10.1109/JIOT.2022.3176394.
- Marques, L., Eugênio, P., Bastos, L., Santos, H., Rosário, D., Nogueira, E., Cerqueira, E., Kreutz, M., and Neto, A. (2023). Analysis of electrical signals by machine learning for classification of individualized electronics on the internet of smart grid things (iosgt) architecture. *Journal of Internet Services and Applications*, 14(1):124–135. DOI: 10.5753/jisa.2023.3076.
- More, P. A. and Patel, Z. M. (2023). Lorawan performance analysis with data rate. In *2023 1st International Conference on Cognitive Computing and Engineering Education (ICCCCEE)*, pages 1–5. IEEE. DOI: 10.1109/ICCCCEE55951.2023.10424626.
- Neto, G. A. S., Da Silva, T. A., Abreu, P. F., Veloso, A. F. D. S., Mendes, L. H. d. O., and Dos Reis, J. V. (2024). Addressing mobility challenges in lorawan through adaptive data rate: A statistical median-based approach. In *2024 11th International Conference on Future Internet of Things and Cloud (FiCloud)*, pages 330–337. IEEE. DOI: 10.1109/FiCloud62933.2024.00058.
- Semtech (2017). Sx1301 datasheet. Available at:<https://tinyurl.com/2tn4zfu6> Accessed: 2025-07-09.
- Soto-Vergel, A., Arismendy, L., Bornacelli-Durán, R., Cardenas, C., Montero-Arévalo, B., Rivera, E., Calle, M., and Candelo-Becerra, J. E. (2023). Lora performance in industrial environments: Analysis of different adr algorithms. *IEEE Transactions on Industrial Informatics*, 19(10):10501–10511. DOI: 10.1109/TII.2023.3240696.
- Veloso, A. F. d. S., Júnior, J. V. R., Rabelo, R. d. A. L., and Silveira, J. D.-f. (2021). Hydsmaas: A hybrid communication infrastructure with lorawan and loramesh for the demand side management as a service. *Future Internet*,

- 13(11):271. DOI: 10.3390/fi13110271.
- Wei, Y., Tsang, K. F., Wang, W., and Zhou, M. M. (2023). Priority-based resource allocation optimization for multi-service lorawan harmonization in compliance with ieee 2668. *Sensors*, 23(5):2660. DOI: 10.3390/s23052660.
- Yang, M.-S. and Hussain, I. (2023). Unsupervised multi-view k-means clustering algorithm. *IEEE Access*, 11:13574–13593. DOI: 10.1109/ACCESS.2023.3243133.
- Zain, A. R., Oktivasari, P., Agustin, M., Kurniawan, A., Murad, F. A., and Nurrahman, I. (2022). Evaluation of encryption and decryption data packet delivery performance in smart home design using the lorawan protocol. In *2022 5th International Conference of Computer and Informatics Engineering (IC2IE)*, pages 241–246. IEEE. DOI: 10.1109/IC2IE56416.2022.9970045.